A Switched-Boost DC/DC Converter with High Voltage Gain and Continuous Input Current

Ali Mostaan[1], Ahmed Abdelhakim[2], Mohsen Soltani[3], Frede Blaabjerg[3]
[1]Iranian Central Oil Field Company, Tehran, Iran
[2]Dept. of Management and Engineering, University of Padova, Vicenza, Italy
[3]Dept. of Energy Technology, Aalborg University, Aalborg, Denmark
Email: ali_8457@yahoo.com, ahmed.a.abdelrazek@ieee.org, sms@et.aau.dk, fbl@et.aau.dk

***Abstract*—A new switched-boost DC/DC converter with high voltage gain is presented in this paper. Compared to other equivalent high voltage gain converters, the proposed converter utilizes less number of passive elements. Moreover, it uses two active switches with the same control signal and it has a shorter commutation paths, resulting in the lowest possible voltage spikes across these switches. In addition, the merit of having a continuous input current in the proposed converter makes it convenient to many applications like the renewable energy systems. The proposed converter is analyzed and compared among its counterparts from different perspectives. Finally, the introduced analysis is verified using simulation and experimental results, where a *200 W* prototype is utilized.**

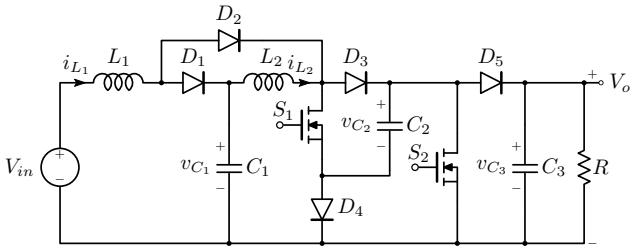

Fig. 1. Proposed high gain step-up DC/DC converter.

I. Introduction

Conventional energy sources, such as oil, natural gas, and coal, have many negative impacts on the environment such as greenhouse impacts and pollution. On the other hand, renewable energy sources, such as photovoltaic (PV) and fuel cell (FC), are cleaner and their penetration into the power system is continuously increasing. In PV and FC-fed power systems, high step-up DC/DC converters are mandatory in order to boost the low output voltage of the PV or the FC, e.g. 20-40 V, to higher voltages, e.g. 200-400 V [1], [2].

Theoretically, the voltage gain of the conventional boost converters can reach infinity. Meanwhile, due to the different parasitics in the experimental layout, this voltage gain can not exceed 4-5 in a well designed layout [3], [4]. Hence, in order to overcome such voltage gain limitation, different solutions have been introduced in literature. The authors in [5] are discussing the merits behind the utilization of the switched-inductor and the switched-capacitor cells in the conventional boost, CUK, SEPIC and ZETA converters. However, the obtained voltage gain may not practically be sufficient for some typical systems. Therefore, several switched-inductor or switched-capacitor cells (i.e. multicell operation) are mandatory in order to reach higher voltage gains, resulting in an increase in the converter size, cost, and complexity [6]–[9].

On the other hand, the use of coupled-inductor is an effective approach to increase the voltage gain practically using less number of components [10]–[12]. Using this approach (i.e. the coupled-inductor approach), the voltage gain can be increased by increasing the coupled-inductor turns ratio without adding extra components. Meanwhile, in order to protect the used switches from the voltage spikes that arise from the leakage inductance, an additional snubber circuit is mandatory to be used. This additional snubber circuit imposes extra losses and complexity in the converter structure [13].

In addition to the prior structures, the Z-source concept has initially been proposed in [14] as a single stage DC/AC power converter. However, this concept can also be used in DC/DC, AC/AC and AC/DC power conversion with minor modifications, as described in [15] for the DC/DC conversion. Despite the seen merits behind the Z-source concept, the initial Z-source network suffers from some demerits such as high inrush current during start-up, discontinuous input current, and limited voltage gain [16]. Accordingly, in order to mitigate the prior problems, several modifications have been adopted on the original Z-source network, such as the quasi Z-source converters [17]–[19], the switched-inductor Z-source converter [20], the enhanced boost Z-source converter [21], and the recently proposed impedance network boost converter [22]. The quasi Z-source converters have the merit of a continuous input current, but the voltage gain capability is similar to the conventional Z-source converter. Meanwhile, the voltage gain has been improved in the other mentioned topologies, but discontinuous input and inrush start-up currents are the major demerits behind these topologies. Furthermore, these Z-source-based converters suffer also from the high number of components. In [23], the enhanced boost quasi Z-source converter has been proposed in order to overcome the discontinuous input and the inrush current problems in the enhanced boost Z-source converter. However, the number of components is still relatively high.

In order to mitigate the aforementioned problems, a new high step-up DC/DC converter is proposed in this paper. The

978-1-5386-1180-7/18/$31.00 ©2018 IEEE

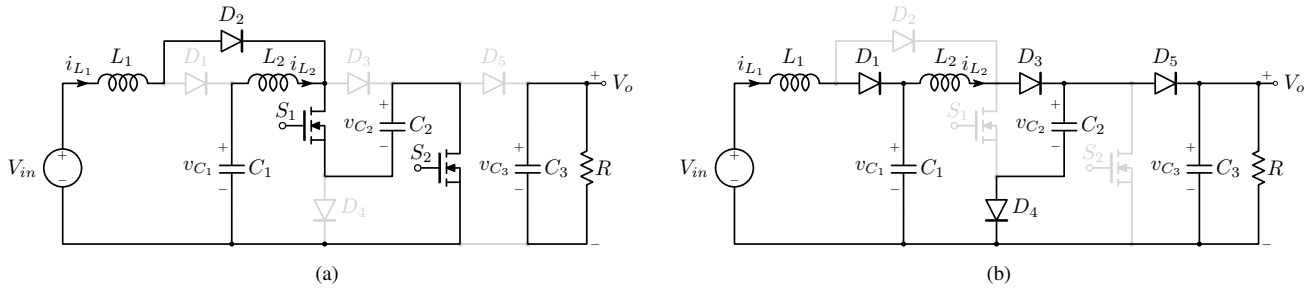

Fig. 2. Modes of operation of the proposed converter. (a) First mode, in which the inductors are charging; and (b) second mode, in which the inductors are discharging.

proposed converter achieves a high voltage gain and draws a continuous input current using less number of components compared to its counterparts. This high voltage gain can be obtained with a small duty cycle in order to prevent the magnetic core saturation as discussed in [22].

The rest of this paper is organized as follows: the proposed converter is analyzed and compared with the state of the art equivalent topologies in Section II. Section III introduces the efficiency analysis of the proposed converter. In Section IV, a 200 W prototype of the proposed converter is designed, simulated, and built experimentally in order to validate the reported analysis and examine its performance. Finally, conclusions are drawn in Section V.

II. Proposed DC/DC Converter

A. Analysis of the Proposed Converter

The proposed converter is shown in Fig. 1 and it comprises two switches, five diodes, two inductors, and three capacitors. In order to analyse the proposed converter the following assumptions are taken:

- all the components are ideal. Therefore the drain-source resistance of the MOSFETs and the forward voltage drop of the diodes are neglected;
- all the capacitors are large enough and the voltage ripple across them is negligible;
- the equivalent series resistance of the passive components is neglected;
- the inductors are large enough to maintain the converter operation in the continuous conduction mode (CCM).

With these assumptions, there are two modes of operation in each switching cycle as shown in Fig. 2, where the inductors are charging in the first mode which is shown in Fig. 2(a), and discharging in the second mode which is shown in Fig. 2(b).

In the first mode as shown in Fig. 2(a), S_1 and S_2 are simultaneously turned ON with the same PWM signal (i.e. the same control signal). Moreover, all the diodes, except D_2, are OFF. In this mode, both inductors (L_1 and L_2) are charging, while C_3 is discharging. In the second mode which is shown in Fig. 2(b), S_1 and S_2 are turned OFF simultaneously, and all the diodes, except D_2, are ON.

Due to the volt-sec balance of the inductors and the charge balance of the capacitors in steady-state, the normalized average voltages across the capacitors (V_{C_1}/V_{in}, V_{C_2}/V_{in}, and V_{C_3}/V_{in}) are given by

$$\frac{V_{C_1}}{V_{in}} = \frac{1-2D}{1-4D+2D^2}, \qquad \frac{V_{C_2}}{V_{in}} = \frac{V_{C_3}}{V_{in}} = \frac{1}{1-4D+2D^2}, \tag{1}$$

where D is the duty cycle of the PWM signal given to S_1 and S_2, and it is equal to t_{ON}/T_s, where t_{ON} is the ON time that corresponds to the first mode and T_s is the time of one switching cycle. Then, the normalized average inductor currents (I_{L_1}/I_{in} and I_{L_2}/I_{in}), being I_{in} is the average dc input current, are given by

$$\frac{I_{L_1}}{I_{in}} = 1, \qquad \frac{I_{L_2}}{I_{in}} = 1-D. \tag{2}$$

It is worth to note that the average output voltage (V_o) is equal to the average voltage across C_3 (V_{C_3}), i.e. the normalized output voltage V_o/V_{in} is given by

$$\frac{V_o}{V_{in}} = \frac{1}{1-4D+2D^2}, \tag{3}$$

which defines the voltage gain (G) of the proposed converter.

In order to properly select the values of the different passive elements in the converter, certain amounts of voltage and current ripples are considered. Then, by defining ΔI_{L_1} and ΔI_{L_2} as the peak-to-peak current ripples of L_1 and L_2 respectively, while defining ΔV_{C_1}, ΔV_{C_2}, and ΔV_{C_3} as the peak-to-peak voltage ripples of C_1, C_2, and C_3 respectively, the passive elements can be selected utilizing the following equations:

$$L_1 = \frac{(1-D)(V_{C_1}-V_{in})}{f_s \cdot \Delta I_{L_1}}, \tag{4}$$

$$L_2 = \frac{(1-D)(V_{C_2}-V_{C_1})}{f_s \cdot \Delta I_{L_2}}, \tag{5}$$

$$C_1 = \frac{D \cdot (1-D) \cdot I_{in}}{f_s \cdot \Delta V_{C_1}}, \tag{6}$$

$$C_2 = \frac{D \cdot (2-D) \cdot I_{in}}{f_s \cdot \Delta V_{C_2}}, \tag{7}$$

$$C_3 = \frac{D \cdot I_o}{f_s \cdot \Delta V_{C_3}}, \tag{8}$$

where f_s is the switching frequency, which is equal to $1/T_s$,

TABLE I
VOLTAGE AND CURRENT STRESSES OF THE DIFFERENT SEMICONDUCTOR DEVICES IN THE PROPOSED CONVERTER

	S_1 and S_2	D_1	D_2	D_3	D_4	D_5
Peak voltage	$G \cdot V_{in}$	$V_{C_1} + V_{C_2}$	$V_{C_2} - V_{C_1}$	$G \cdot V_{in}$		
Peak current	$I_{L_1} + \Delta I_{L_1}/2 +$ $I_{L_2} + \Delta I_{L_2}/2$	$I_{L_1} + \Delta I_{L_1}/2$		$I_{L_2} + \Delta I_{L_2}/2$	$I_{L_2} + \Delta I_{L_2}/2 -$ $I_o/(1-D)$	$I_o/(1-D)$

TABLE II
COMPARISON AMONG THE PROPOSED CONVERTER AND THE STATE OF THE ART CONVERTERS INTRODUCED IN [20]–[25]

	Proposed converter	Converter in [20]	Converter in [21]	Converter in [22]	Converter in [23]	Converter in [24]	Converter in [25]
Num. of switches	2	1	1	1	1	2	2
Num. of diodes	5	8	6	8	6	5	6
Num. of inductors	2	4	4	4	4	2	2
Num. of capacitors	3	3	5	3	5	3	2
Input current continuity	Yes	No	Yes	No	Yes	Yes	No
Input and output grounds	Common	Not common	Not common	Common	Common	Not common	Not common

TABLE III
PARAMETERS OF THE IMPLEMENTED 200 W SWITCHED-BOOST DC/DC CONVERTER

V_{out}	300 V	f_s	100 kHz
V_{in}	30 V	L_1	360 μH
C_1	2.2 μF	L_2	360 μH
C_2	2.2 μF	C_3	2.2 μF

and I_o is the average output current.

Table I summarizes the voltage and current stresses of the different semiconductor devices. Note that the voltage ripples across the different capacitors are assumed to be negligible.

B. Comparative Study

In order to evaluate the performance of the proposed converter, a comparative study with the state of the art equivalent topologies is considered. Fig. 3 shows the voltage gain of the proposed converter (i.e. V_o/V_{in}) compared with the equivalent topologies introduced in [20]–[25]. Furthermore, Table II introduces a comparison among the proposed converter and the prior mentioned state of the art converters in terms of number of switches, diodes, and passive elements, and input current continuity.

According to Fig. 3, it can be seen that the voltage gain of the proposed converter is higher than the converter presented in [20], [22], [24], [25] and similar to the converters presented in [21], [23]. Meanwhile, compared to the latter converters (i.e. the converters presented in [21], [23]), the proposed converter utilizes less diodes and passive elements but with an additional switch as shown in Table II. Furthermore, unlike the converter presented in [21], the proposed converter benefits from having a common ground between the input and the output.

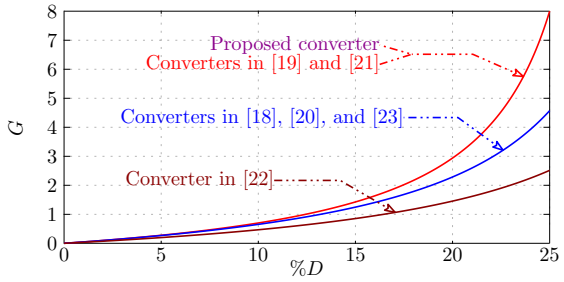

Fig. 3. Voltage gain versus duty cycle variation of the proposed high gain step-up DC/DC converter versus the equivalent converters.

III. EFFICIENCY ANALYSIS

In order to analyse the converter efficiency the following assumptions are made:

1) capacitors are large enough. Therefore, the voltage ripple across them is negligible;
2) inductors current ripple is negligible;
3) switches ON resistances are modeled with r_{DS1} and r_{DS2} for S_1 and S_2, respectively and their parasitic capacitances are represented with C_{S1} and C_{S2} respectively;
4) V_{F1}, V_{F2}, V_{F3}, V_{F4}, and V_{F5} represent the forward voltages of D_1, D_2, D_3, D_4, and D_5 respectively;
5) R_{L1}, R_{L2}, and R_{L3} are the equivalent series resistance of L_1, L_2 and L_3, respectively.

The conduction losses of the switches can be calculated by

$$P_{r_{DS1}} = r_{DS1} I^2_{rms_{S1}} = r_{DS1} D (I_{L1} + I_{L1})^2 = r_{DS1} D (2-D)^2 I_{in}, \quad (9)$$

$$P_{r_{DS2}} = r_{DS2} I^2_{rms_{S2}} = r_{DS2} D (I_{L1} + I_{L1})^2 = r_{DS2} D (2-D)^2 I_{in}. \quad (10)$$

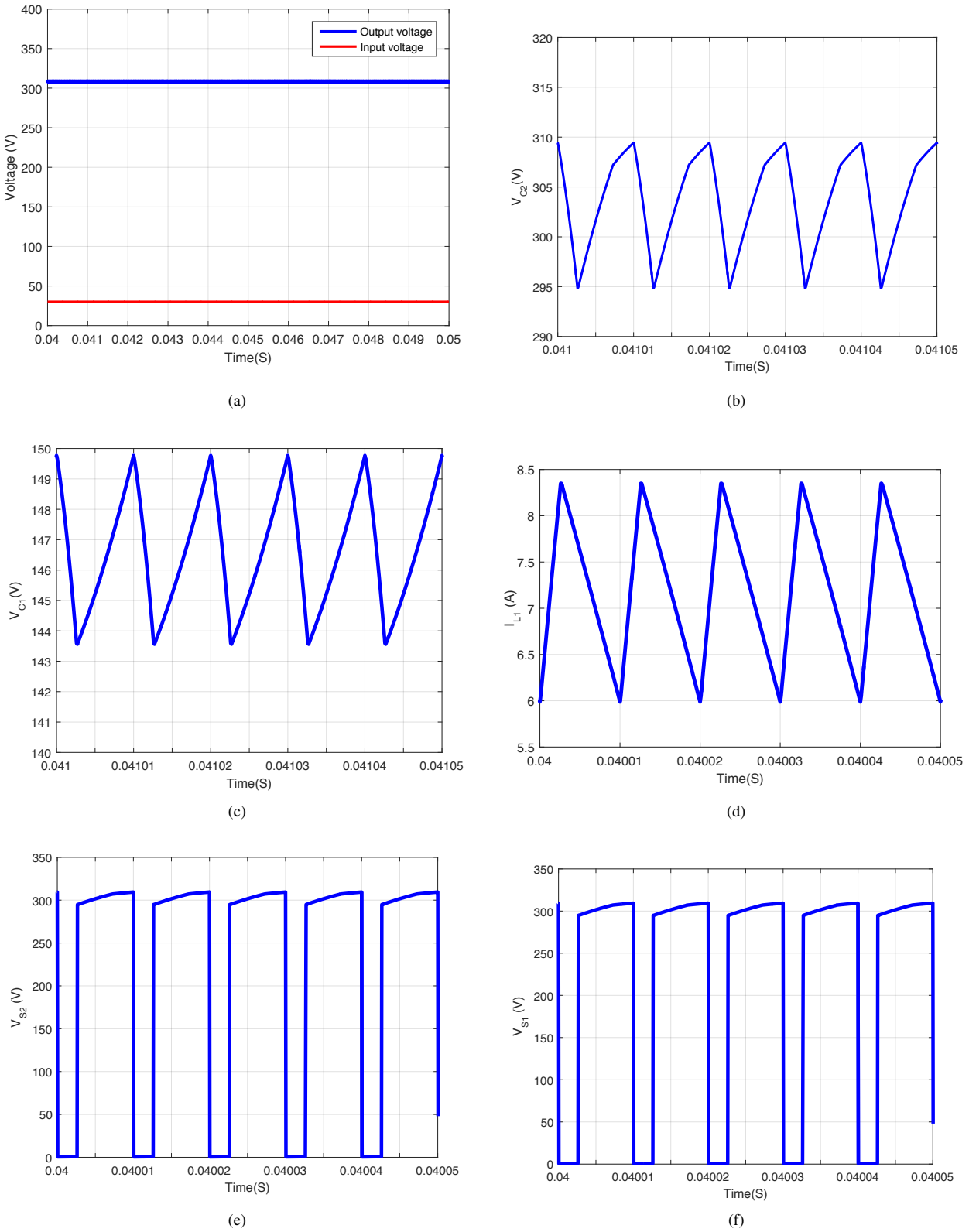

Fig. 4. Simulation waveforms of the proposed converter at full-load (a) input and output voltage (b) voltage across C2 (c) voltage across C1 (d) input current (e) switch S1 voltage (f) switch S2 voltage

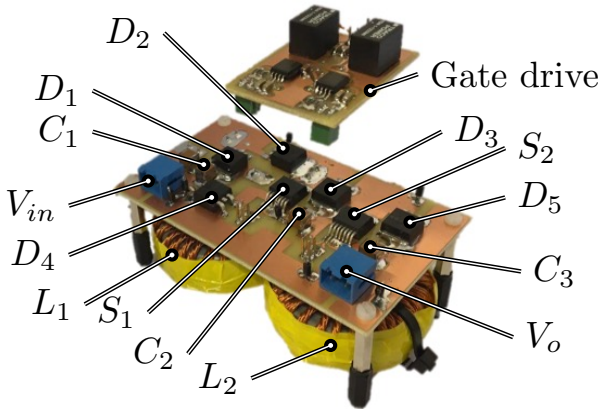

Fig. 5. 200 W switched-boost DC/DC converter.

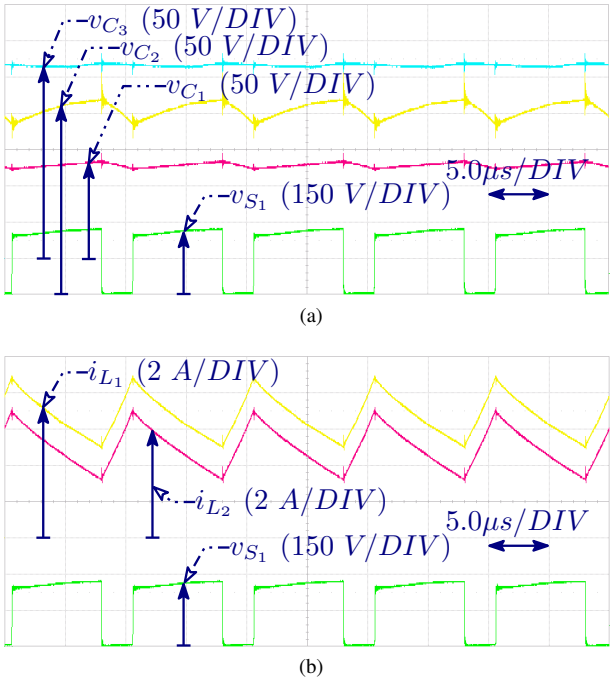

Fig. 6. Experimental results of the 200 W switched-boost DC/DC converter. (a) Voltages across the different capacitors and the voltage across S_1 as well; and (b) shows the currents in L_1 and L_2 in addition to the voltage across S_1. Note that the voltage gain is equal to 10.

Meanwhile, the switching losses can be obtained from

$$P_{S1} = C_{S1} f_s V_{S1}^2 = C_{S1} f_s V_O^2, \tag{11}$$

$$P_{S2} = C_{S2} f_s V_{S2}^2 = C_{S2} f_s V_O^2, \tag{12}$$

where, V_{S1} and V_{S2} are the voltage stress across S_1 and S_2, respectively. Then, the diodes conduction loss can be calculated as follows:

$$\begin{aligned} P_{D1} &= V_{F1} I_{ave_{D1}} = (1-D) V_{F1} I_{L1} \\ &= (1-D) V_{F1} I_{in}, \end{aligned} \tag{13}$$

$$\begin{aligned} P_{D2} &= V_{F2} I_{ave_{D2}} = D V_{F1} I_{L1} \\ &= D V_{F1} I_{in}, \end{aligned} \tag{14}$$

$$\begin{aligned} P_{D3} &= V_{F3} I_{ave_{D3}} = (1-D) V_{F3} I_{L2} \\ &= (1-D)^2 V_{F3} I_{in}, \end{aligned} \tag{15}$$

$$\begin{aligned} P_{D4} &= V_{F4} I_{ave_{D4}} = D V_{F3} (I_{L1} + I_{L2}) \\ &= (2-D) V_{F3} I_{in}, \end{aligned} \tag{16}$$

$$P_{D4} = V_{F5} I_{ave_{D5}} = (1-D) V_{F5} I_o. \tag{17}$$

The conduction losses in the inductors can be estimated from

$$P_{L1} = R_{L1} I_{L1}^2 = R_{L1} I_{in}^2, \tag{18}$$

$$P_{L2} = R_{L2} I_{L2}^2 = (1-D) R_{L1} I_{in}^2. \tag{19}$$

Finally, the total power loss of the proposed converter can be calculated from

$$\begin{aligned} P_{loss} =& \Sigma_{i=1}^{2} P_{r_{DS_i}} + \Sigma_{i=1}^{2} P_{S_i} \\ &+ \Sigma_{i=1}^{5} P_{D_i} + \Sigma_{i=1}^{2} P_{L_i}. \end{aligned} \tag{20}$$

Therefore, the converter efficiency can be written as

$$\eta = \frac{P_O}{P_{in}} = \frac{P_O}{P_O + P_{loss}}. \tag{21}$$

IV. Simulation and Experimental Results

In order to verify the theoretical results, the converter is simulated using a MATLAB/Simulink model. The circuit parameters are as given in Table III. The output voltage is about 300 V as is shown in Fig. 4(a) which is consistent with (4). The voltages across C_2 and C_3 are shown in Fig. 4(b)-(c), respectively. The voltage ripple across C_2 is about 15 V, i.e. about 5% of its nominal voltage (300 V). The voltage across C_1 is oscillating between 143 V and 150 V and its voltage ripple is lower than 5% of its nominal voltage (145 V). The input current is shown in Fig. 4(d). It is can be seen that the input current is continuous and its ripple is about 28%. The voltage stresses of S_1 and S_2 are shown in Fig. 4(e)-(f), respectively. The voltage stress on both switches is equal to output voltage, which is consistent with theoretical results.

In order to verify the prior analysis and examine the functionality of the proposed converter, a 200 W prototype is designed and implemented as shown in Fig. 5, whose parameters are listed in Table III.

The experimental results of this prototype are shown in Fig. 6(a) and Fig. 6(b), where Fig. 6(a) shows the voltages across the different capacitors and the voltage across S_1 as well, while Fig. 6(b) shows the currents in L_1 and L_2 in addition to the voltage across S_1. Note that the inductors have higher current ripples than the theoretical value due to the higher voltage ripples across the capacitors. These results confirms the functionality of the proposed converter and verifies the reported analysis.

V. Conclusion

In this paper, a new DC/DC converter with high voltage gain and continuous input current capabilities has been proposed.

This converter utilizes less number of passive elements compared to the equivalent converters. The proposed converter is analyzed and the design procedure of the passive elements is introduced. Moreover, a comparative study among this converter and the state of the art equivalent topologies is presented. Finally, simulation and experimental results of a 200 W system have been shown.

REFERENCES

[1] F. Blaabjerg, K. Ma, and Y. Yang, "Power electronics - the key technology for renewable energy systems," in *Ninth International Conf. on Ecological Vehicles and Renewable Energies (EVER)*, March 2014, pp. 1–11.

[2] M. Forouzesh, Y. P. Siwakoti, S. A. Gorji, F. Blaabjerg, and B. Lehman, "Step-up dc-dc converters: A comprehensive review of voltage-boosting techniques, topologies, and applications," *IEEE Transactions on Power Electronics*, vol. 32, no. 12, pp. 9143–9178, Dec 2017.

[3] A. A. Fardoun and E. H. Ismail, "Ultra step-up dc-dc converter with reduced switch stress," *IEEE Trans. on Industry App.*, vol. 46, no. 5, pp. 2025–2034, Sept 2010.

[4] A. Abdelhakim, P. Mattavelli, P. Davari, and F. Blaabjerg, "Performance evaluation of the single-phase split-source inverter using an alternative dc-ac configuration," *IEEE Trans. Ind. Electron.*, vol. PP, no. 99, pp. 1–1, 2017.

[5] B. Axelrod, Y. Berkovich, and A. Ioinovici, "Switched-capacitor/switched-inductor structures for getting transformerless hybrid dc-dc pwm converters," *IEEE Trans. on Circuits and Syst. I: Reg. Papers*, vol. 55, no. 2, pp. 687–696, March 2008.

[6] Y. Tang, T. Wang, and D. Fu, "Multicell switched-inductor/switched-capacitor combined active-network converters," *IEEE Trans. on Power Electron.*, vol. 30, no. 4, pp. 2063–2072, April 2015.

[7] Y. Tang, D. Fu, T. Wang, and Z. Xu, "Hybrid switched-inductor converters for high step-up conversion," *IEEE Trans. on Ind. Electron.*, vol. 62, no. 3, pp. 1480–1490, March 2015.

[8] M. Prudente, L. L. Pfitscher, G. Emmendoerfer, E. F. Romaneli, and R. Gules, "Voltage multiplier cells applied to non-isolated dc-dc converters," *IEEE Trans. on Power Electron.*, vol. 23, no. 2, pp. 871–887, March 2008.

[9] J. C. Rosas-Caro, J. M. Ramirez, F. Z. Peng, and A. Valderrabano, "A dc-dc multilevel boost converter," *IET Power Electron.*, vol. 3, no. 1, pp. 129–137, January 2010.

[10] Y. Tang, D. Fu, J. Kan, and T. Wang, "Dual switches dc/dc converter with three-winding-coupled inductor and charge pump," *IEEE Trans. on Power Electron.*, vol. 31, no. 1, pp. 461–469, Jan 2016.

[11] X. Hu, G. Dai, L. Wang, and C. Gong, "A three-state switching boost converter mixed with magnetic coupling and voltage multiplier techniques for high gain conversion," *IEEE Trans. on Power Electron.*, vol. 31, no. 4, pp. 2991–3001, April 2016.

[12] L. S. Yang, T. J. Liang, H. C. Lee, and J. F. Chen, "Novel high step-up dc-dc converter with coupled-inductor and voltage-doubler circuits," *IEEE Trans. on Ind. Electron.*, vol. 58, no. 9, pp. 4196–4206, Sept 2011.

[13] Y. P. Siwakoti, F. Blaabjerg, and P. C. Loh, "High step-up trans-inverse (tx^{-1}) dc-dc converter for the distributed generation system," *IEEE Trans. on Ind. Electron.*, vol. 63, no. 7, pp. 4278–4291, July 2016.

[14] F. Z. Peng, "Z-source inverter," *IEEE Trans. on Ind. Appl.*, vol. 39, no. 2, pp. 504–510, Mar 2003.

[15] V. P. Galigekere and M. K. Kazimierczuk, "Analysis of pwm z-source dc-dc converter in ccm for steady state," *IEEE Trans. on Circuits and Systems I: Reg. Papers*, vol. 59, no. 4, pp. 854–863, April 2012.

[16] A. Abdelhakim, P. Mattavelli, and G. Spiazzi, "Three-phase split-source inverter (ssi): Analysis and modulation," *IEEE Transactions on Power Electronics*, vol. 31, no. 11, pp. 7451–7461, Nov 2016.

[17] Y. Zhang, J. Shi, L. Zhou, J. Li, M. Sumner, P. Wang, and C. Xia, "Wide input-voltage range boost three-level dc-dc converter with quasi-z source for fuel cell vehicles," *IEEE Trans. on Power Electron.*, vol. 32, no. 9, pp. 6728–6738, Sept 2017.

[18] M. M. Haji-Esmaeili, M. Naseri, H. Khoun-Jahan, and M. Abapour, "Fault-tolerant and reliable structure for a cascaded quasi-z-source dc-dc converter," *IEEE Trans. on Power Electron.*, vol. 32, no. 8, pp. 6455–6467, Aug 2017.

[19] A. Abdelhakim, P. Davari, F. Blaabjerg, and P. Mattavelli, "Switching loss reduction in the three-phase quasi-z-source inverters utilizing modified space vector modulation strategies," *IEEE Transactions on Power Electronics*, vol. PP, no. 99, pp. 1–1, 2017.

[20] M. Zhu, K. Yu, and F. L. Luo, "Switched inductor z-source inverter," *IEEE Trans. on Power Electron.*, vol. 25, no. 8, pp. 2150–2158, Aug 2010.

[21] H. Fathi and H. Madadi, "Enhanced-boost z-source inverters with switched z-impedance," *IEEE Trans. on Ind. Electron.*, vol. 63, no. 2, pp. 691–703, Feb 2016.

[22] G. Zhang, H. H. C. Iu, B. Zhang, Z. Li, T. Fernando, S. Z. Chen, and Y. Zhang, "An impedance network boost converter with a high-voltage gain," *IEEE Trans. on Power Electron.*, vol. 32, no. 9, pp. 6661–6665, Sept 2017.

[23] V. Jagan, J. Kotturu, and S. Das, "Enhanced-boost quasi-z-source inverters with two switched impedance network," *IEEE Trans. on Ind. Electron.*, vol. PP, no. 99, pp. 1–1, 2017.

[24] M. H. B. Nozadian, E. Babaei, S. H. Hosseini, and E. S. Asl, "Steady-state analysis and design considerations of high voltage gain switched z-source inverter with continuous input current," *IEEE Trans. on Ind. Electron.*, vol. PP, no. 99, pp. 1–1, 2017.

[25] E. Babaei, E. S. Asl, M. H. Babayi, and S. Laali, "Developed embedded switched-z-source inverter," *IET Power Electron.*, vol. 9, no. 9, pp. 1828–1841, 2016.